Short communication

Effect of contact type between anode and carbonaceous fuels on direct carbon fuel cell reaction characteristics

Chen Li, Yixiang Shi, Ningsheng Cai *

Key Laboratory for Thermal Science and Power Engineering of Ministry of Education, Department of Thermal Engineering, Tsinghua University, Beijing 100084, China

ARTICLE INFO

ABSTRACT

The contact between the anode and the carbonaceous fuel has a strong effect on the direct carbon fuel cell (DCFC) reaction characteristics. These effects are experimentally investigated by measuring the electrochemical behavior of a detached anode, an anode in physical contact with the fuel and an anode with carbon deposited on the surface in a DCFC. The results show that for the detached type DCFC, the reaction characteristics are closely related to the anode gas. In an Ar atmosphere, the main anode reactions are the electrochemical reaction to produce O_2 and the carbon gasification with the formed O_2. In a CO_2 atmosphere, the main anode reactions are the carbon gasification with CO_2 and the electrochemical oxidization of the formed CO. For the physical contact type DCFC, the anode reaction mechanisms are the same as for the detached type DCFC with no electrochemical oxidization of carbon at the physical contact interface between the carbonaceous fuel and the anode. Thus, the increased contact does not result in better performance. The carbon-deposited type DCFC has better performance with a significant activation polarization due to the electrochemical oxidization of the deposited carbon.

1. Introduction

The direct carbon fuel cell (DCFC) is widely regarded as one of the most promising technologies for power generation. The DCFC has a higher theoretical efficiency [1] and can utilize easily achieved carbonaceous fuel [2]. DCFCs are classified into three types according to the electrolyte as molten hydroxide [2–6], molten carbonate [7–14] and solid oxide electrolyte [15–24] fuel cells. In addition, studies have been conducted combining the molten carbonate and solid oxide electrolytes together to obtain better performances [25–27]. The present study focuses on the solid oxide electrolyte DCFC, which has a relatively higher reaction activity due to its higher operating temperatures and which eliminates liquid electrolyte consumption, leakage and corrosion.

Zahradnik et al. [28] first proposed a system with the coal gasification unit combined with a solid oxide fuel cell (SOFC). Nakagawa and Ishida [15] placed charcoal in the anode chamber of a button cell, using N_2 as the anode gas to test the DCFC performance and claimed that the fuel cell was driven by carbon monoxide produced by the charcoal gasification. The reactions in the anode were listed as [15]:

$$C + CO_2 \leftrightarrow 2CO \tag{1}$$

$$O^{2-} + CO \leftrightarrow CO_2 + 2e^- \tag{2}$$

Eq. (1) is the gasification reaction of carbonaceous fuel, which is known as the Boudouard reaction. Eq. (2) is the electrochemical reaction of CO, which occurs at the anode three-phase boundary. In 1992, Gür and Huggins [16] placed solid carbon adjacent to an yttria-stabilized zirconia (YSZ) tube, using He as the anode gas, with the cell and carbonaceous fuel temperatures controlled independently. The current density was about $70\,A\,m^{-2}$ at 0.6 V for a 955 °C cell and 932 °C carbon. They reported that the reactions in the anode were:

$$2O^{2-} \leftrightarrow O_2 + 4e^- \tag{3}$$

$$C + O_2 \leftrightarrow CO_2 \text{ or } 2C + O_2 \leftrightarrow 2CO \tag{4}$$

The reactions expressed by Eqs. (3) and (4) only take place when the residual active gases are negligible in the anode chamber. In the experiments of Nakagawa and Ishida [15] and Gür and Huggins [16], the anode and the carbonaceous fuel were detached, while the experiments had no direct electrochemical reactions of the carbonaceous fuel in the DCFC, with the carbon gasification reactions and then the gaseous electrochemical reactions in the anode.

Chuang [29] directly placed the carbonaceous fuel on the anode in a SOFC and obtained about $1000\,A\,m^{-2}$ current density at 0.6 V, 950 °C. They reported that the electrochemical oxidization of carbon took place at the contact surface between the anode and the

* Corresponding author. Tel.: +86 10 62789955; fax: +86 10 62789955.
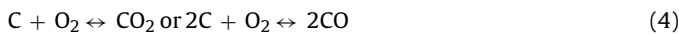 *E-mail address:* cains@tsinghua.edu.cn (N. Cai).

carbonaceous fuel as:

$$C + 2O^{2-} \leftrightarrow CO_2 + 4e^- \qquad (5)$$

Recently, Liu et al. [19] developed a DCFC by filling a conventional anode-supported tubular SOFC with commercial carbon black. The maximum power densities were 1040, 750 and 470 W m^{-2} at 850 °C, 800 °C and 750 °C, respectively. The chemical and electrochemical reactions in the anode during discharging were assumed as:

$$C + 2O^{2-} \leftrightarrow CO_2 + 4e^- \qquad (5)$$

$$C + CO_2 \leftrightarrow 2CO \qquad (1)$$

$$O^{2-} + CO \leftrightarrow CO_2 + 2e^- \qquad (2)$$

They reported that the oxygen ions reacted with the carbon only when the carbon was in intimately contact with the anode surface with the reactions in Eqs. (1) and (2) as the dominant anodic reactions, which determined the cell performance. In 2007, Li et al. [17] employed a SOFC based fluidized bed configuration to convert solid carbon directly into electricity. They setup fluidized carbon particles in the reactor, so the carbon particles could then contact the fuel cell anode. The maximum power density was about 430 W m^{-2} at 900 °C. They reported that there was no electrochemical oxidization of the carbon with the reactions in the He fluidizing environment:

$$2O^{2-} \leftrightarrow O_2 + 4e^- \qquad (3)$$

$$C + O_2 \leftrightarrow CO_2 \text{ or } 2C + O_2 \leftrightarrow 2CO \qquad (4)$$

$$C + CO_2 \leftrightarrow 2CO \qquad (1)$$

$$O^{2-} + CO \leftrightarrow CO_2 + 2e^- \qquad (2)$$

Eq. (3) is the disassociation of the molecular oxygen at the anode, which then chemically oxidizes the carbon particle to form CO or CO$_2$ (Eq. (4)). The CO formation expressed by Eq. (1) is thermodynamically more favored at 900 °C. Any CO that is formed during this reaction is electrochemically oxidized to CO$_2$ at the three-phase boundary (Eq. (2)). Use of CO$_2$ as the fluidizing gas instead of He significantly improved the DCFC performance, which further proved the reaction mechanism. The produced CO$_2$ is often recycled to the anode to increase the carbonaceous fuel gasification rate to improve the DCFC performance. In the experiments of Chuang [29], Liu et al. [19] and Li et al. [17], the anode and the carbonaceous fuel were in physical contact. There are some disputes about the reactions for the physical contact conditions in previous studies as mentioned above, with the main focus on whether electrochemical oxidization of the carbon occurs at the contact interface.

Ihara et al. [21–24] proposed a rechargeable direct carbon fuel cell (RDCFC), that differed fundamentally from the detached or physical contact designs with employed the deposited carbon as the fuel. The deposited carbon was supplied by thermal decomposition of propane or methane at the anode. In this case, the carbonaceous fuel deposited in the porous anode would be in contact with the ionic conductor, the electron conductor or the three-phase boundary; therefore, the electrochemical oxidization of carbon occurred during the power generation as described by:

$$C + 2O^{2-} \leftrightarrow CO_2 + 4e^- \qquad (5)$$

or

$$C + O^{2-} \leftrightarrow CO + 2e^- \qquad (6)$$

Once the CO was produced, it reacted with O^{2-} and then acted as the fuel instead of the carbon in the DCFC.

The existing solid oxide electrolyte DCFCs can then be classified into three types according to the type of contact between the anode and the carbonaceous fuel as detached from the anode [15,16], in physical contact with the anode [17,19,29] or deposited carbon contact [21–24] type DCFCs. The anode reactions are closely related to the contact type, which significantly affects the DCFC reaction characteristics. However, previous DCFC studies have used very different carbonaceous fuels, cell materials, geometries and operating conditions; thus, it is difficult to evaluate the effects of contact type on the DCFC reaction characteristics.

This study analyzes the electrochemical behavior of the detached, the physical contact and the carbon-deposited contact type DCFCs with the other conditions kept constant. The effects of the contact between the anode and the carbonaceous fuel on the DCFC reaction characteristics are analyzed based on experimental results.

2. Experiments

2.1. Anode-supported button cell

Button cells have been widely used in DCFC experiments due to there simple test setup and good repeatability [15,21–24,29–31]. This study used anode-supported SOFC button cells made by SIC-CAS (Shanghai Institute of Ceramics, Chinese Academy of Sciences). The cells consisted of a Ni/YSZ anode support layer (680 μm), a Ni/scandium-stabilized zirconium (ScSZ) anode active interlayer (15 μm), a ScSZ electrolyte layer (20 μm), and a lanthanum strontium manganate (LSM)/ScSZ cathode layer (15 μm) [31]. The cathode layer was 1.4 cm in diameter and all other layers were 2.6 cm in diameter. The button cells used in the present study were cut from one large cell plate so the anode and electrolyte layers of all cells were assumed to be homogeneous; thus eliminating the anodic material differences caused by cell to cell variations in fabrication. Before testing, silver paste was spread on the anode and cathode surfaces by screen-printing for current collection. Fig. 1 shows the exterior appearance of the button cells before the tests.

2.2. Test setup and experimental conditions

Fig. 2 shows a schematic of the test setup used for evaluating the DCFC performance. The button cell was located at the end of two concentric alumina tubes and pressed against an alumina plate, which was constrained by springs. The Pt mesh was used as the cathode current collector and was fixed to the porous cathode. The
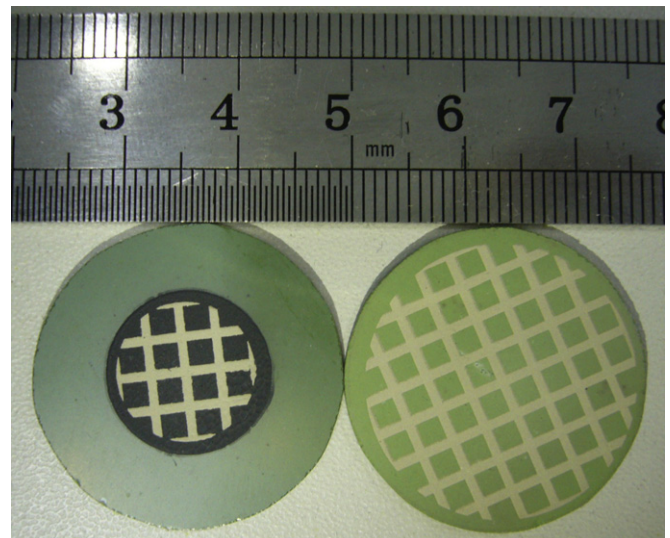

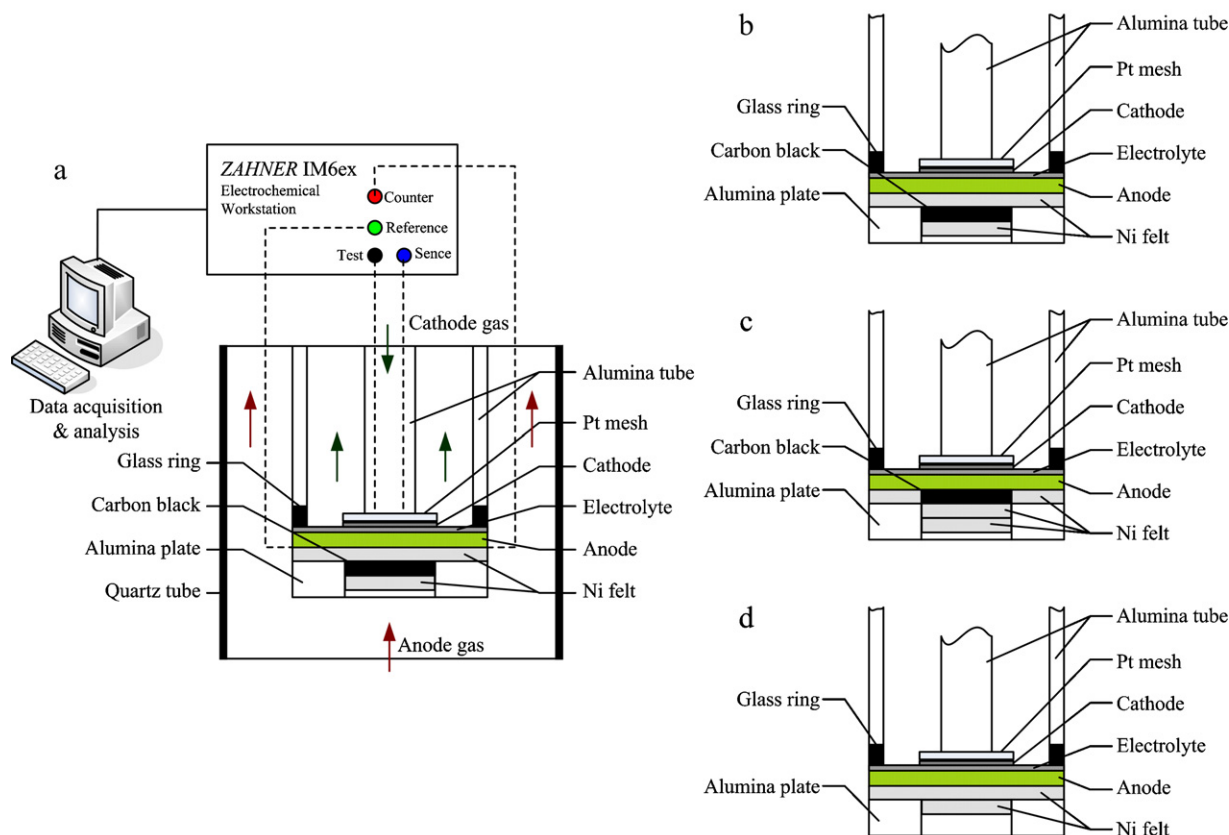**Fig. 1.** Exterior appearance of button cells before the tests.

Fig. 2. Schematics of the test setup for the (a) entire test device and various contact type DCFCs including (b) detached, (c) physical contact and (d) carbon-deposited.

oxidant flowed in the inner tube to the cathode and passed through the porous Pt mesh. A porous Ni felt was fixed to the anode support layer to collect the anode current. Pt wires were used on both electrodes as voltage and current probes. A borosilicate glass ring (SiO$_2$ 76%, B$_2$O$_3$ 15%, R$_2$O 6%, Al$_2$O$_3$ 3%, Beijing Glass Instrument Factory, China) was used as sealant to separate the anode and cathode gases. All the devices were enclosed in a quartz tube and heated by a furnace kept at a constant operating temperature.

A 1.6 cm diameter hole was drilled into the alumina plate center to arrange the carbonaceous fuel. Commercial carbon black (Black Pearls 2000, GP-3848, Cabot Corporation, USA) was used as the fuel after being crushed to 150–200 μm particles. The carbon black arrangements differed for the three DCFC contact types. As shown in Fig. 2(b), 50 mg carbon black was placed between the two Ni felt layers for the detached type DCFC. The upper Ni felt layer was used to collect the anodic current while the lower layer supported the carbon black. The physical contact type DCFC used an annular current collection Ni felt with 50 mg carbon black in direct contact with the anode (Fig. 2(c)). The test setup for the carbon-deposited contact type DCFC was similar to that for the detached type DCFC but without the carbon black arrangement (Fig. 2(d)). The deposited carbon was supplied by thermal decomposition of CH$_4$ at the anode. Two layers of Ni felt were used for all the cases to eliminate the possible differences of gas diffusion with the anode gas diffusing easily to the anode due to the porous (porosity 95%) Ni felt.

During the tests, the button cell temperature was held at 800 °C with air used as the oxidant at a flowrate of 100 ml min^{-1}. Pure H$_2$ was fed into the chamber for 1 h at a flowrate of 100 ml min^{-1} to fully reduce the anode. The electrochemical characteristics of the DCFCs were measured using the four-probe method with an electrochemical workstation (IM6ex, Zahner-Elektrik GmbH, Germany).

Both the detached and the physical contact type DCFCs used pure Ar and CO$_2$ as the anode gas. The polarization curves were measured after the cell was attached to an open circuit for 30 min (Case I) and after the cell was discharging at 0.5 V for 5 min (Case II). For the carbon-deposited contact type DCFC, the button cell was attached to an open circuit using 100 ml min^{-1} CH$_4$ as the anode gas after reducing by H$_2$ and purging by Ar. After the carbon deposition from the CH$_4$ cracking, the anode gas was switched to pure Ar at 200 ml min^{-1} and the anode chamber was purged for 30 min. Then, the polarization curves and the constant current discharge curve were measured. When the cell voltage during the constant current discharge process decreased to 0 V, the button cell circuit was opened and the furnace operating temperature was reduced to the ambient temperature at 1.5 °C min^{-1}.

3. Results and discussion

3.1. Reaction characteristics of the detached type DCFC

The polarization curves of the detached type DCFC are shown in Fig. 3. The results show that the anode gas significantly affects the reaction characteristics. Theoretically, the carbon gasification reactions and gaseous electrochemical reactions in the detached type DCFC occur in the anode without direct electrochemical oxidization of the carbon.

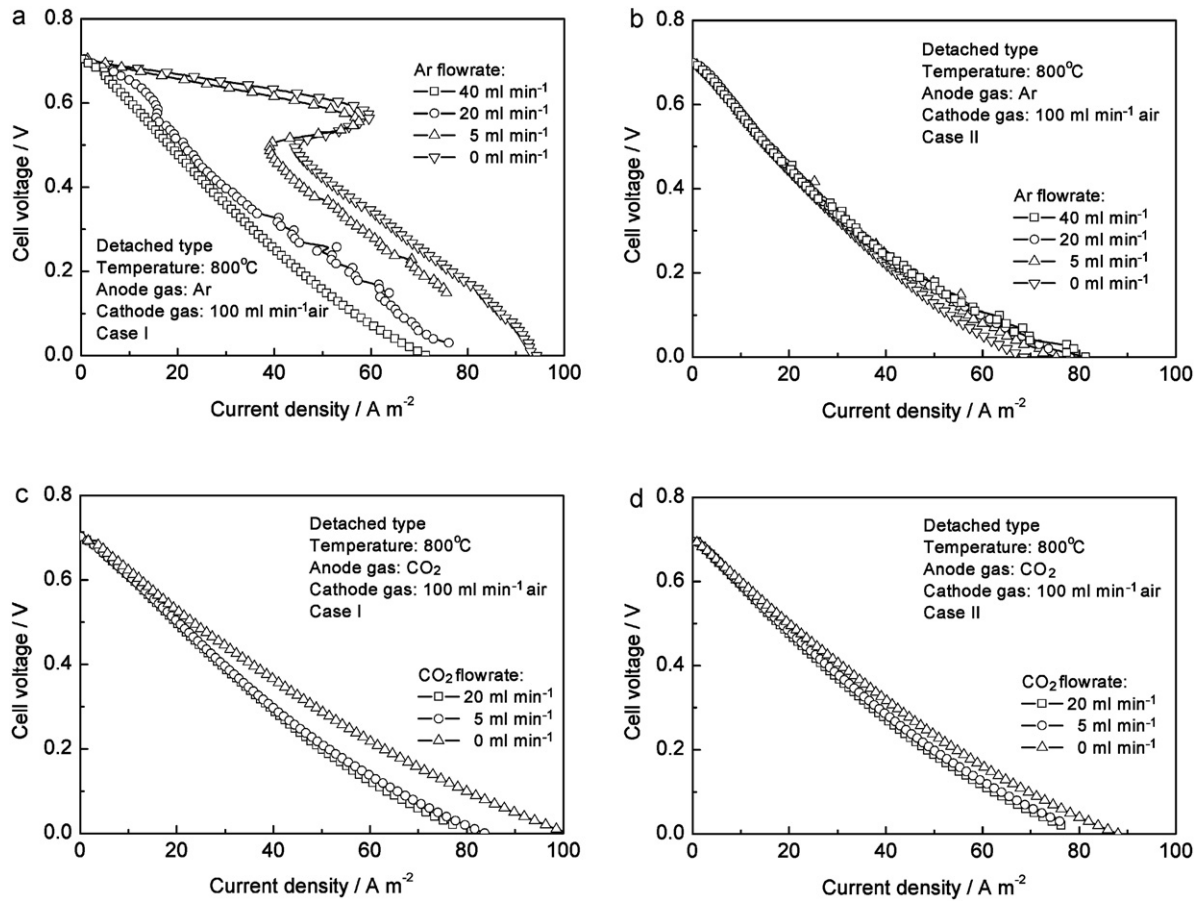When Ar was used as the anode gas, the reactions in the anode are as:

$$2O^{2-} \leftrightarrow O_2 + 4e^- \tag{3}$$

$$C + O_2 \leftrightarrow CO_2 \text{ or } 2C + O_2 \leftrightarrow 2CO \tag{4}$$

$$O^{2-} + CO \leftrightarrow CO_2 + 2e^- \tag{2}$$

Fig. 3. Polarization curves for the detached type DCFC: (a) Ar Case I, (b) Ar Case II, (c) CO_2 Case I and (d) CO_2 Case II.

The molecular oxygen produced by the electrochemical reaction at the anode then chemically oxidizes the carbon to form CO or CO_2. Any formed CO is electrochemically oxidized to CO_2 at the three-phase boundary. The CO_2 concentration produced in the reaction is very low due to the dilution by Ar in the anode chamber. The Boudouard reaction expressed by Eq. (1) is almost insignificant at 800 °C with a low CO_2 concentration. This anode reaction mechanism is then fully consistent with the reaction characteristics in Fig. 3(a) and (b). When the cell was attached to an open circuit for 30 min (Case I), there was no current and the electrochemical reaction did not occur in the anode. The O_2 concentration was low but CO accumulated at a relatively high concentration. The polarization curves were measured by linearly reducing the cell voltage from the open circuit voltage to 0 V at a rate of $10\,mV\,s^{-1}$. Then, the formed CO took part in the electrochemical reaction and the current density increased with decreasing cell voltage. The quick consumption of the produced CO reduces the cell performance at some point in the polarization curve testing process, as can be seen in Fig. 3(a). The twist in the polarization curve is obvious only at low Ar flowrates ($0–5\,ml\,min^{-1}$). At high flowrates ($\geq 20\,ml\,min^{-1}$) the Ar significantly dilutes the CO, which impairs the cell performance and eliminates the twist in the polarization curve. Similarly, the CO consumption during the continuous discharging in Case II results in the polarization curve being similar to that in Case I at high flowrates. The cell performance in both cases decreases with increasing Ar flowrate.

When CO_2 is used as the anode gas, the CO_2 reacts with the carbon with the produced CO taking part in the electrochemical oxidization reaction as:

$$C + CO_2 \leftrightarrow 2CO \tag{1}$$

$$O^{2-} + CO \leftrightarrow CO_2 + 2e^- \tag{2}$$
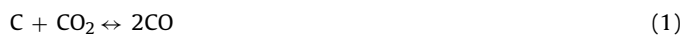
Meanwhile, the reaction expressed in Eq. (1) reached equilibrium due to excessive CO_2 in the anode chamber and the CO concentration became steady. Therefore, common polarization curves were observed in Case I with CO_2 as the anode gas (Fig. 3(c)). Comparison of Fig. 3(c) and (d) indicates that continuous charging has little effect on the CO concentration at the same CO_2 flowrate. In addition, the cell performance is enhanced with increasing CO_2 flowrate, unlike with Ar as the anode gas. These results further prove that the dominant anode reactions in DCFC are different in Ar and CO_2 atmospheres.

3.2. Reaction characteristics for the physical contact type DCFC

The polarization curves for the physical contact type DCFC shown in Fig. 4 are similar to those in Fig. 3, indicating that the electrochemical behavior of the physical contact type DCFC is similar to that of the detached type DCFC when the other conditions are held the same. The small difference in performance is mainly caused by the different ohmic resistances.

The direct electrochemical oxidation of carbon occurs only at a certain anodic overpotential, which then results in a significant activation polarization in the cell polarization curve. However, comparison to the detached type DCFC shows no obvious activation polarization nor performance enhancement due to the electrochemical oxidation of carbon in the polarization curves for the physical contact type DCFC. Therefore, these macro reaction characteristics suggest that no electrochemical reaction of carbon take place at the physical contact interface between the carbonaceous fuel and the anode and if the reaction even exists, the propor-
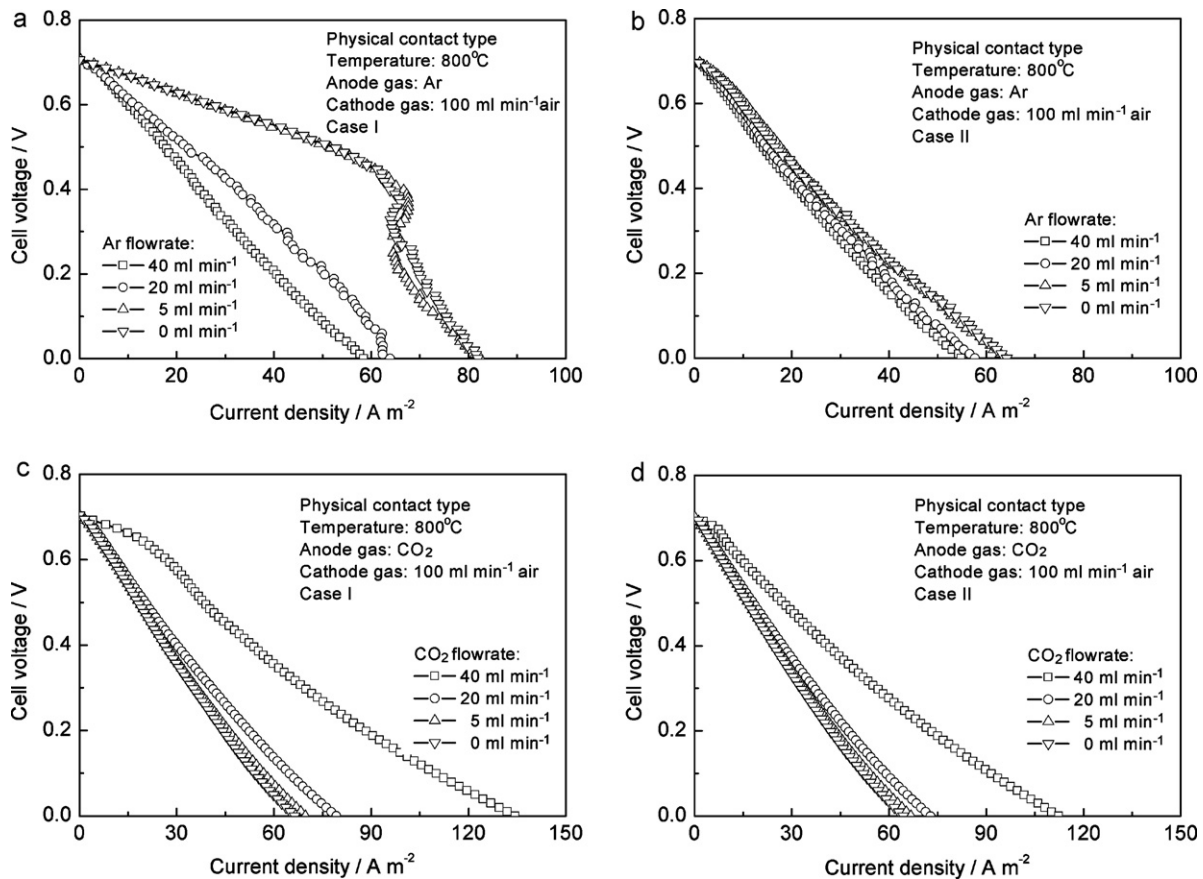
Fig. 4. Polarization curves of the physical contact type DCFC: (a) Ar Case I, (b) Ar Case II, (c) CO_2 Case I and (d) CO_2 Case II.

tion is so small that its contribution to the cell performance can be neglected. A previous study [32] showed that direct electrochemical oxidation of carbon requires that O^{2-} in the anode ionic conductor contact a carbon reactive site with the released electron conducted to the external circuit. This reaction condition is extremely unlikely for the physical contact type DCFC. Therefore, the anode reaction mechanism in the physical contact type DCFC is the same as in the detached type DCFC and increasing the contact between the carbonaceous fuel and the anode will not improve the cell performance.

3.3. Reaction characteristics of the carbon-deposited contact type DCFC

The polarization curves of the carbon-deposited contact type DCFC are shown in Fig. 5. Comparison of the results in Figs. 3(a), 4(a) and 5 shows that these three types of DCFCs have very different electrochemical behaviors for the same operating conditions. First, the DCFC performance is much better in Fig. 5. During discharging of the carbon-deposited contact type DCFC, all the deposited carbon at the three-phase boundary and on the YSZ and Ni particle surfaces can participate in the electrochemical reactions [32]. The deposited carbon is also close enough to the three-phase boundary so that the electrochemical oxidization of the deposited carbon can easily take place. However, in the detached and the physical contact type DCFCs, the slower carbon gasification reactions and diffusion processes restrict the gaseous electrochemical reactions. Therefore, the cell performance of the carbon-deposited type DCFC is significantly higher than that of the detached type and physical contact type DCFCs. Secondly, the activation polarizations are seen to affect the curves in the high cell voltage region in
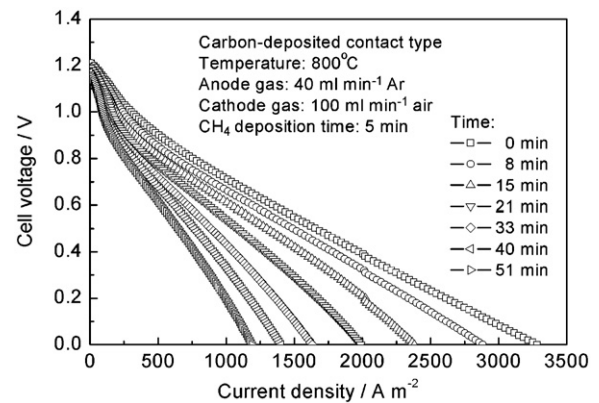

Fig. 5. Polarization curves of the carbon-deposited contact type DCFC.

Fig. 5, which indicates that the electrochemical oxidation of carbon requires a certain anodic overpotential. The proportion of the activation polarization in the total polarization of the carbon-deposited type DCFC is higher than in the detached type or physical contact type DCFCs. The current density at each voltage decreases and the activation polarization overpotential increases with increasing reaction time and with the consumption of the deposited carbon in the anode. As the cell voltage approaches 0 V, the electrochemical reaction is more difficult for the residual carbon deposited in the anode. Thirdly, for the 40 ml min^{-1} Ar anode gas flowrate, the polarization curve is not twisted in Figs. 3(a), 4(a) or 5.

The constant current discharge curve at $300\,A\,m^{-2}$ for the carbon-deposited contact type DCFC is given in Fig. 6. The discharge curve is similar to that in the Hasegawa et al. [24] experiments. At
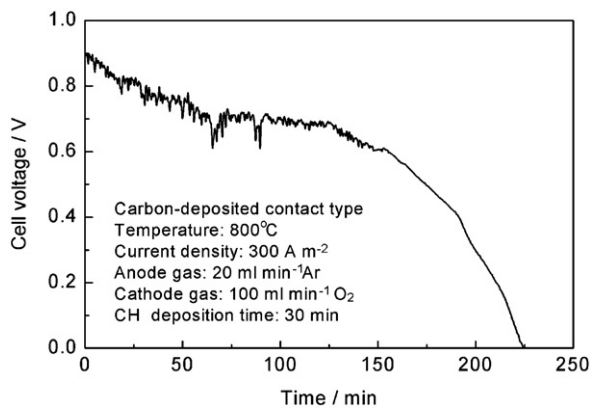
Fig. 6. Constant current discharge curve for the carbon-deposited contact type DCFC.

the beginning of the discharge process, the cell voltage fluctuates greatly. The cell voltage then decreases gradually with time. The cell voltage decreases more quickly after 200 min to 0 V as shown in Fig. 6. Then, the residual deposited carbon in the anode can no longer sustain the 300 A m^{-2} current density. A more detailed mechanism for the carbon direct electrochemical reactions in the carbon-deposited contact DCFC was given by Li et al. [32].

4. Conclusions

This study experimentally investigates the effects of the contact type between the anode and the carbonaceous fuel on the DCFC reaction characteristics. The DCFC electrochemical behavior was measured for detached fuel, fuel in physical contact with the anode and carbon-deposited contact direct carbon fuel cells (DCFC). The results show that for the detached type DCFC, the reaction characteristics closely depend on the anode gas. The main anode reactions are the electrochemical reaction to produce O_2 and carbon gasification with the formed O_2 in an Ar atmosphere, and the carbon gasification with CO_2 and the electrochemical oxidization of the formed CO in a CO_2 atmosphere. Any CO formed with Ar as the anode gas is electrochemically oxidized to CO_2 at the three-phase boundary. Thus, the Ar flowrate and the discharge step strongly affect the cell electrochemical behavior. For the physical contact type DCFC, the anode reaction mechanism is the same as for the detached type DCFC with no electrochemical reaction involving the carbon at the physical contact interface between the carbonaceous fuel and the anode. Thus, the increased physical contact does not improve the cell performance. The carbon-deposited type DCFC has better performance with a significant activation polarization due to the electrochemical oxidization of the deposited carbon.

References

[1] S. Basu, Recent Trends in Fuel Cell Science and Technology, Anamaya, New Delhi, 2007.
[2] S. Zecevic, E.M. Patton, P. Parhami, Carbon 42 (2004) 1983–1993.
[3] T.A. Edison, US 460,122 (1891).
[4] W.W. Jacques, US 555,511 (1896).
[5] G.A. Hackett, J.W. Zondlo, R. Svensson, J. Power Sources 168 (2007) 111–118.
[6] T. Nunoura, K. Dowaki, C. Fushimi, S. Allen, E. Meszaros, M.J. Antal, Ind. Eng. Chem. Res. 46 (2007) 734–744.
[7] W.H.A. Peelen, M. Olivry, S.F. Au, J.D. Fehribach, K. Hemmes, J. Appl. Electrochem. 30 (2000) 1389–1395.
[8] J.F. Cooper, R. Krueger, N. Cherepy, US 6,815,105 B2 (2004).
[9] J.R. Selman, J. Power Sources 160 (2006) 852–857.
[10] M. Steinberg, Int. J. Hydrogen Energy 31 (2006) 405–411.
[11] X. Li, Z. Zhu, J. Chen, R. de Marco, A. Dicks, J. Bradley, G. Lu, J. Power Sources 186 (2009) 1–9.
[12] H. Li, Q. Liu, Y. Li, Electrochim. Acta 55 (2010) 1958–1965.
[13] M. Chen, C. Wang, X. Niu, S. Zhao, J. Tang, B. Zhu, Int. J. Hydrogen Energy 35 (2010) 2732–2736.
[14] D. Cao, G. Wang, C. Wang, J. Wang, T. Lu, Int. J. Hydrogen Energy 35 (2010) 1778–1782.
[15] N. Nakagawa, M. Ishida, Ind. Eng. Chem. Res. 27 (1988) 1181–1185.
[16] T.M. Gur, R.A. Huggins, J. Electrochem. Soc. 139 (1992) L95–L97.
[17] S. Li, A.C. Lee, R.E. Mitchell, T.M. Gur, Solid State Ionics 179 (2008) 1549–1552.
[18] T.M. Gur, M. Homel, A.V. Virkar, J. Power Sources 195 (2010) 1085–1090.
[19] R. Liu, C. Zhao, J. Li, F. Zeng, S. Wang, T. Wen, Z. Wen, J. Power Sources 195 (2010) 480–482.
[20] J. Kim, H. Lim, C. Jeon, Y. Chang, K. Koh, S. Choi, J. Song, J. Power Sources 195 (2010) 7568–7573.
[21] M. Ihara, K. Matsuda, H. Sato, C. Yokoyama, Solid State Ionics 175 (2004) 51–54.
[22] M. Ihara, S. Hasegawa, J. Electrochem. Soc. 153 (2006) A1544–A1546.
[23] H. Saito, S. Hasegawa, M. Ihara, J. Electrochem. Soc. 155 (2008) B443–B447.
[24] S. Hasegawa, M. Ihara, J. Electrochem. Soc. 155 (2008) B58–B63.
[25] S.L. Jain, Y. Nabae, B.J. Lakeman, K.D. Pointon, J.T.S. Irvine, Solid State Ionics 179 (2008) 1417–1421.
[26] K. Pointon, B. Lakeman, J. Irvine, J. Bradley, S. Jain, J. Power Sources 162 (2006) 750–756.
[27] A.S. Lipilin, I.I. Balachov, L.H. Dubois, A. Sanjurjo, M.C. McKubre, S. Crouch-Baker, M.D. Hornbostel, F.L. Tanzclla, US 2007/0269688 A1 (2007).
[28] R.L. Zahradnik, L. Elikan, D.H. Archer, in: G.J. Young, H.R. Linden (Eds.), Fuel Cell Systems, vol. 47, American Chemical Society, Washington, DC, 1965, pp. 343–356.
[29] S.S.C. Chuang, Carbon-based Fuel Cell, Akron, 2006.
[30] Y. Wu, C. Su, C. Zhang, R. Ran, Z. Shao, Electrochem. Commun. 11 (2009) 1265–1268.
[31] C. Li, Y. Shi, N. Cai, J. Power Sources 195 (2010) 4660–4666.
[32] C. Li, Y. Shi, N. Cai, J. Power Sources 196 (2011) 754–763.